Subharmonic Oscillation Modeling and MISO Volterra Series

Otilia M. Boaghe and Stephen A. Billings

***Abstract*—Subharmonic generation is a complex nonlinear phenomenon which can arise from nonlinear oscillations, bifurcation and chaos. It is well known that single-input–single-output Volterra series cannot currently be applied to model systems which exhibit subharmonics. A new modeling alternative is introduced in this paper which overcomes these restrictions by using local multiple input single output Volterra models. The generalized frequency-response functions can then be applied to interpret systems with subharmonics in the frequency domain.**

***Index Terms*—Bifurcations, chaos, frequency-response functions, nonlinear oscillations, response spectrum map, subharmonics, Volterra series.**

I. Introduction

THE steady-state output of a linear system driven by a sine wave will consist of a sine wave of the same frequency but with a different amplitude and phase. Nonlinear systems driven by a sine wave may produce new frequency components, including components at integer multiples of the input frequency called harmonics, or new frequency components at fractions of the input frequency, called subharmonics.

An important practical problem of nonlinear systems which is particularly evident in mechanical systems is subharmonic dynamics. In many industrial fields an important issue is the possibility of controlling subharmonics. Examples of real situations in which subharmonic generation can be a critical problem are given for example in Lefschetz [11], Nayfeh and Mook [12], Ishida *et al.* [9], or Ishida [10]. A theoretical interest in studying subharmonics emerged over the last few decades from the connection between chaos and subharmonics. It has been noticed [6], [18] that subharmonic generation is the first step on the route to chaos. Therefore, studying subharmonics may provide more insight into the phenomenon of chaos.

Motivated by theoretical and practical importance, subharmonic oscillations have been studied not only in nonlinear vibration theory, but also in the context of nonlinear systems, dynamical systems applications and control [16]. Very often, the tools employed for analysis belong to differential geometry and topological vector spaces, especially when the subharmonics are associated with bifurcations and chaos [8]. However, new methods of identification and analysis which allow subharmonic systems to be easily studied are needed before controller design procedures can be investigated and developed.

In this paper, the main objective is to introduce a new way of modeling and interpreting systems which exhibit subharmonics. For such systems, single-input–single-output (SISO) Volterra models cannot currently be used to model systems which can produce subharmonic oscillations. A new modeling approach is introduced in this paper which overcomes these restrictions by using local multiple-input–single-output (MISO) Volterra models. The advantage of the new approach is that all the existing knowledge regarding the interpretation, analysis, and properties of Volterra models can be applied to reveal new insights into subharmonic systems. In particular, the generalized frequency-response functions (GFRFs) which are the frequency-domain equivalents of the Volterra kernels can be used to study subharmonic systems in the frequency domain.

The paper is organized as follows. In Section II, the theoretical background to the Volterra series in both time and frequency domain is briefly reviewed. The main definitions and properties for subharmonic oscillations are summarized in Section III. In Section IV, a new modeling methodology is introduced for subharmonic systems, based on MISO Volterra series. This methodology is applied to the Duffing–Ueda and Duffing–Holmes oscillators. The simulation examples described in this paper show that combining subharmonic modeling with the nonlinear GFRFs or transfer-function generation may indeed reveal new features of a system exhibiting subharmonics. The new modeling principle is expected to improve the understanding of the complex problem of subharmonic and chaos generation.

II. Volterra Series in Time and Frequency Domain

The importance of the Volterra series became apparent when Wiener [17] applied the Volterra series to an investigation of a nonlinear circuit response by relating the system input $u(t)$ to the output $y(t)$ by a functional series given by

$$y(t) = \sum_{n=1}^{\infty} y_n(t) = \sum_{n=1}^{\infty} \int_{-\infty}^{\infty}\int_{-\infty}^{\infty}\cdots\int_{-\infty}^{\infty} h_n(\tau_1,\tau_2,\ldots,\tau_n) \times \prod_{i=1}^{n} u(t-\tau_i)d\tau_i. \quad (1)$$

Manuscript received April 3, 2002; revised October 15, 2002. The work of O. M. Boaghe was supported by the University of Sheffield, U.K. The work of S. A. Billings was supported by the Engineering and Physical Sciences Research Council (EPSRC). This paper was recommended by Associate Editor A. Ushida.

O. M. Boaghe was with the Department of Automatic Control and Systems Engineering, University of Sheffield, Sheffield S1 3JD, U.K. She is now with Philips Semiconductors, Zurich CH-8045, Switzerland.

S. A. Billings is with the Department of Automatic Control and Systems Engineering, University of Sheffield, Sheffield S1 3JD, U.K. (e-mail: s.billings@sheffield.ac.uk).

Digital Object Identifier 10.1109/TCSI.2003.813965

The quantities $h_n(\tau_1, \tau_2, \ldots, \tau_n)$ in (1) are known as *kernels of order* n, or the nth*-order impulse response functions* of the system.

The initial studies on Volterra series addressed fundamental issues such as existence, convergence and uniqueness. In practical problems only a finite Volterra series can be used, also called a *truncated Volterra series* or *polynomial Volterra series*. In particular, Boyd and Chua [4] concluded that systems with fading memory may be approximated arbitrarily well by truncated Volterra series. The condition of *fading memory* is a stronger version of continuity [4], [15]. Generally speaking, a system with fading memory is one for which the dependence on the input decreases rapidly enough with time. The fading memory requirement however means that the class of systems with multiple equilibria [4] cannot be represented by a single Volterra model. For these systems, a valid unique global Volterra series representation will not exist. An example is the Duffing oscillator which has more than one equilibrium point in general and in consequence a global unique Volterra series to represent the dynamics around all these points at the same time does not exist.

From the nonlinear-system-analysis perspective, the Volterra series kernels are very useful in describing the system input-output behavior and in finding system properties in a manner which is independent of the input. The Volterra kernels are usually studied in the frequency domain, where almost all types of useful mathematical operations in the time-domain are transformed into algebraic operations. The Fourier transform of the kernels $h_n(\tau_1, \ldots, \tau_n)$ in the Volterra series (1) H_n is called the nth*-order GFRF* of the system [7]

$$H_n(j\omega_1, \ldots, j\omega_n) = \int_{-\infty}^{\infty} \ldots \int_{-\infty}^{\infty} h_n(\tau_1, \ldots, \tau_n) \times e^{-(j\omega_1\tau_1 + \ldots + j\omega_n\tau_n)} d\tau_1 \ldots d\tau_n. \quad (2)$$

The GFRF can also be found in the literature with the name *frequency-domain Volterra kernel* [3], or *nonlinear transfer function* [5]. It is the generalized response function representation which is used in this paper to interpret, analyze and understand a state with subharmonics.

III. Subharmonics: Definitions and Terminology

Nonlinear systems in the presence of forced oscillations and under suitable conditions admit subharmonics as a steady-state solution. Subharmonics are components where the frequency is an integral submultiple of the driving frequency. Subharmonic oscillations have been encountered in many types of systems, including systems which are parametrically excited, stationary or nonstationary. Subharmonics have been detected in both nonlinear discrete systems with finite degrees of freedom and in continuous systems (beams, strings, plates, membranes) with infinite degrees of freedom. Many terms have been associated with subharmonic phenomena, including frequency demultiplication ([12]), subharmonic resonance ([16]), and subharmonic oscillation ([16], [14]).

A direct application of Volterra series in the study of subharmonics is not possible as long as systems with subharmonics have infinite memory, and therefore they do not belong to the Volterra class of systems. In the Section IV, a new methodology is proposed in an attempt to overcome several restrictions associated with existing methods for modeling systems with subharmonics. The new approach is based on using the MISO Volterra models and will be illustrated using the Duffing oscillator. The new models are then further analyzed in both the time and the frequency domain to illustrate the simplicity and advantages of the new approach.

IV. Modeling Subharmonics With MISO Volterra Series

As noted above, it is impossible to model subharmonics with the SISO Volterra series, because the Volterra series respond to a periodic excitation with a periodic signal with the same period. However, if the given input could be modified somehow to create an input with a period equal to the subharmonic oscillation, the Volterra series modeling could be applied. In this section, the possibility of modeling subharmonics with the MISO Volterra series is investigated for the first time.

It is well known that initial conditions are crucially important for a subharmonic to exist in a nonlinear system. Consequently, subharmonics cannot be produced in a Volterra system, where the dependence on the initial conditions gradually fades out. However, the local Volterra series can be derived for a particular steady state of the system. If a local Volterra series representation exists for a state of the system which features subharmonics, then, the local Volterra series will not be expected to be equal to another local Volterra series, corresponding to a different state of that system.

The modified input which could be used for Volterra series modeling of a subharmonic should have the same period as the subharmonic. If the subharmonic considered for modeling has the period n times the original input period T, a modified input u_{mod} should have the period n times the real input period. The modified input can then be considered to be n dimensional, $u_{\text{mod}} = [u_1; \ldots; u_i; \ldots; u_n]$, with the ith component u_i taken as

$$u_i(t) = \begin{cases} 0, & t \in [0; T) \\ \ldots & \\ u(t), & t \in [(i-1)T; iT) \\ 0, & t \in [iT; (i+1)T) \\ \ldots & \\ 0, & t \in [(n-1)T; nT). \end{cases} \quad (3)$$

Consequently, for the individual components $u_i(t)$ it can be verified that

$$u_1(t) + \ldots + u_i(t) + \ldots + u_n(t) = u(t) \quad (4)$$

$$u_i(t) = u_1(t - iT). \quad (5)$$

To allow for MISO Volterra modeling, the system which generates subharmonics in the steady state y when excited with the input u should have the internal structure given in Fig. 1. The information required for modeling is the order n of the subharmonic and the period T of the input signal u. This information can be readily obtained by analysing the system, in the form of a given model or from a system identification study (e.g., a

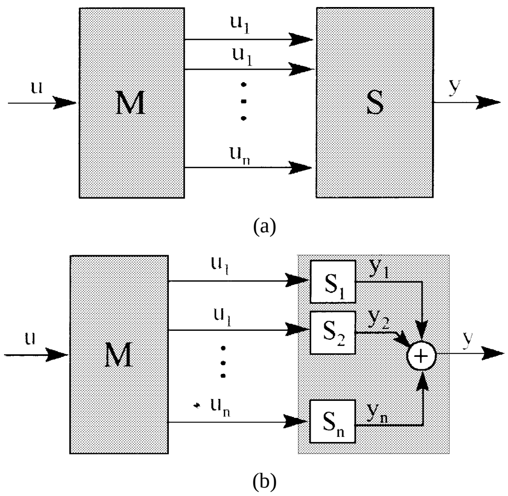

Fig. 1. Internal structure of a nonlinear system generating subharmonics for modeling with (a) MISO Volterra series; (b) MISO Volterra series without cross-product $u_i u_j$ terms.

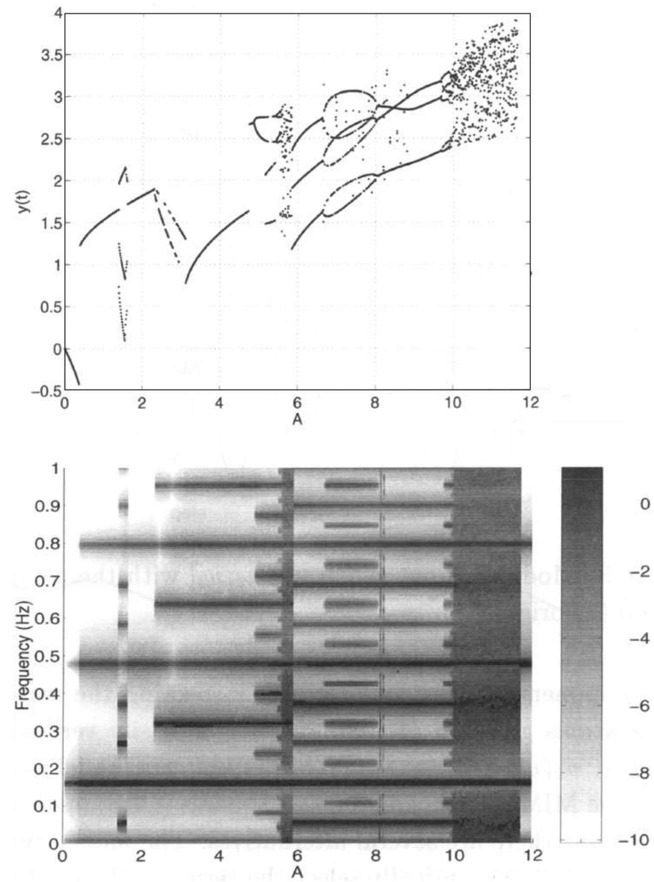

Fig. 2. Bifurcation diagram and response spectrum map (plan view) for the Duffing–Ueda (6).

NARMAX model) using a bifurcation diagram and a response spectrum map. This was illustrated in the examples given in Billings and Boaghe [1] and will be used in the examples below.

The system given in Fig. 1(a) is composed of a time multiplexor M and a MISO system S. The time multiplexor generates the n-dimensional input $u_{\mathrm{mod}} = [u_1; \ldots; u_n]$, based on the original input $u(t)$, the subharmonic order n, and input period T. The modified input u_{mod} is applied to the system S, for which the output is the subharmonic $y(t)$. For the system S, both input u_{mod} and output y have the period nT. Therefore, a local MISO Volterra model can be identified directly from the data generated from the simulation.

To simplify the internal system mechanism the Volterra series to be derived can be prevented from containing cross-product terms of the type $u_i u_j$, $i \neq j$, so that individual contributions from every input u_i can be separated in the Volterra model. If individual contributions at the input are separated, the system S in Fig. 1(b) can be decomposed into n independent subsystems $S_1, \ldots, S_n$, one for every individual input u_i. In this case, the MISO Volterra model will not contain cross-product terms between inputs and the GFRFs can then easily be derived for the individual subsystems S_i.

To summarize, the modeling procedure is given below.

1) Detect a subharmonic steady state using the bifurcation diagram for a simulated implicit difference or differential equation, or any other model form.
2) Identify the order n and the period of oscillation nT of the subharmonic $y(t)$, by visual inspection or using the response spectrum map [1].
3) Generate an n-dimensional modified input u_{mod} based on the original input $u(t)$, using a time multiplexor.
4) Identify a MISO discrete-time Volterra model for the system with output $y(t)$ and the n-dimensional modified input u_{mod}.

The methodology given above for modeling with the MISO Volterra series will be applied in the next section to the Duffing equation, where subharmonics can be generated for example by the Duffing–Ueda or Duffing–Holmes cases. For both cases, the input considered is a periodic sine wave, however the modeling procedure given above is not limited to sine waves. The Volterra series are obtained in the time domain as MISO models based on just the input or exogenous variables, and the Volterra kernels are further analyzed in the frequency domain. To illustrate the ideas in the simplest way, all the examples below start from an assumed known differential equation model of the system. However, the method is based on simulations of the system model for the input u_{mod} and can therefore be just as easily applied to an identified NARMAX, neural networks, or any other model that represents the system.

A. Example 1: Duffing–Ueda Equation

In this example, the Duffing equation is considered in the form also known as the Duffing–Ueda model

$$\ddot{y} + \alpha \dot{y} + y^3 = u(t). \tag{6}$$

For the present analysis, the Duffing–Ueda (6) was simulated for $\alpha = 0.1$ and $u(t) = A\cos(t)$, where $0 \leq A \leq 12$. A fourth-order Runge–Kutta algorithm with an integration interval of $\pi/3000$ was used to simulate the response of the system to the sinusoidal input. The input and output signals were further sampled at periods of $T_s = \pi/60$ s.

For this equation, various dynamic regimes were noticed, for different amplitudes of the input signal. The bifurcation diagram and the response spectrum map, for a varying amplitude A of the

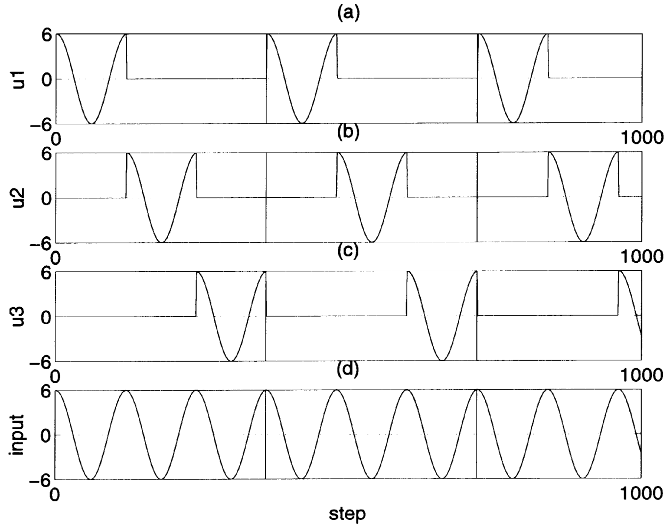

Fig. 3. Modified input signal $[u_1; u_2; u_3]$ with the components: (a) u_1; (b) u_2; (c) u_3; (d) original input.

input signal $u(t) = A\cos(t)$, are given in Fig. 2. The response spectrum map shows that the frequency of the sinusoidal input $f = 1/2\pi = 0.159$Hz is present for all input values A and that subharmonic generation is evident for certain sets of amplitude values. In this example, the subharmonic of order $1/n = 1/3$ at 0.053 Hz obtained for amplitude $A = 6$ in the model (6) will be considered.

In order to derive a Volterra MISO model, a modified input is produced. The modified input is generated from the original input signal, knowing the order of the subharmonic n and the time period T. Both n and T parameters can be readily obtained from the response spectrum map given in Fig. 2. For the amplitude value $A = 6$, the order is $n = 3$ and the time period is $T = 2\pi = 6.28$s. Fig. 3 shows the original input u and the modified three-dimensional input, with the components u_1, u_2 and u_3. By inspecting the waveforms given in Fig. 3, the relations given in (4) and (5) can be easily verified. For a system with the input $[u_1; u_2; u_3]$ a discrete-time MISO Volterra model was identified. In the present study the multiple-input–multiple-output (MIMO) orthogonal least-squares (OLS) method [2] was applied but there are several alternatives. The main advantage of the OLS method is that it can automatically select the terms in the model. Notice that because the MISO consists of a set of Volterra models which only involve the inputs, bias which can be induced by noise should not be a problem and the estimation is therefore relatively straightforward.

Volterra models with three, five, and seven orders of nonlinearity were estimated, providing correspondingly increased degrees of accuracy. For a third order of nonlinearity the model predicted output was already very good, therefore the model selected for further analysis was a third-order MISO Volterra model

$$\begin{aligned} y_1(k) = &-0.6685 + 1.6766u_1(k-3) + 0.8832u_1^2(k-3) \\ &-1.4688u_1(k-1) + 0.0213u_1^3(k-1) \\ &-0.0239u_1^3(k-3) + 0.0048u_1(k-1)u_1^2(k-2) \\ &+0.3323u_1^2(k-1) - 1.1966u_1(k-1)u_1(k-3) \end{aligned} \quad (7)$$

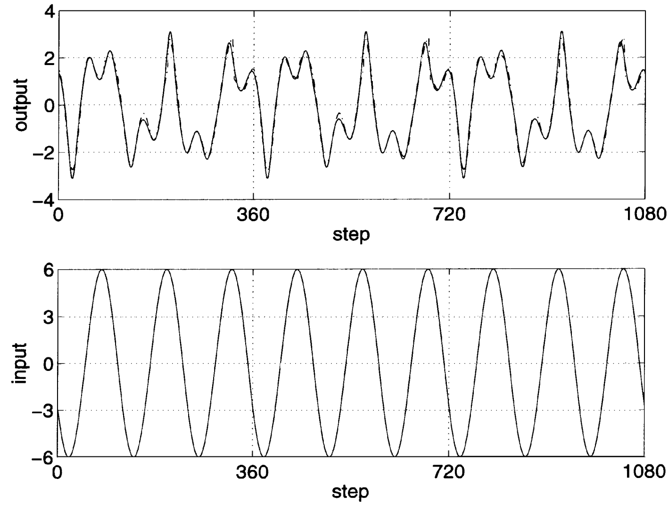

Fig. 4. Model (10) predicted output (dashed line), original output (solid line), and input signal.

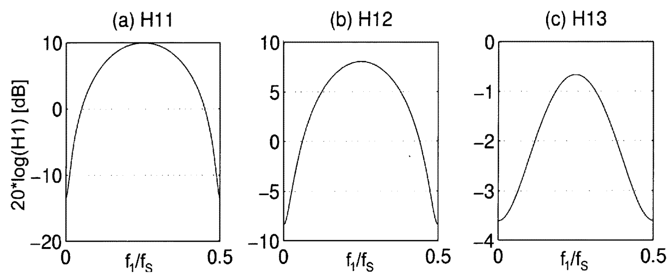

Fig. 5. GFRF $H_1(j\omega)$ for (a) u_1; (b) u_2; (c) u_3 in (10).

$$\begin{aligned} y_2(k) = &\,0.0195u_2^3(k-3) - 1.2882u_2^2(k-3) \\ &-1.0715u_2(k-3) - 1.0424u_2^2(k-1) \\ &+2.3687u_2(k-1)u_2(k-3) \\ &-0.0202u_2^3(k-1) + 1.4514u_2(k-1) \end{aligned} \quad (8)$$

$$\begin{aligned} y_3(k) = &-0.9846u_3^3(k-3) + 0.6732u_3(k-1)u_3^2(k-3) \\ &-0.1331u_3(k-3) + 0.7935u_3(k-1) \\ &+1.0905u_3(k-1)u_3(k-2)u_3(k-3) \\ &+5.7359u_3^2(k-3) + 6.0159u_3^2(k-1) \\ &-11.754u_3(k-1)u_3(k-3) - 0.7903u_3^3(k-1) \end{aligned} \quad (9)$$

where

$$y(k) = y_1(k) + y_2(k) + y_3(k). \quad (10)$$

It should be noticed that according to the general internal structure given in Fig.1 (b), the model has no cross-product input terms (no terms of the type u_1u_2), therefore, the identification procedure is easier, and consists of fitting three SISO Volterra models which are further combined to give the system output. The model predicted output is plotted in Fig. 4, where it can be compared with the original output. Here, the original input signal is also shown, with a period three times smaller than the resulting subharmonic. They match almost exactly and some improvement is obtained for an increased order of nonlinearity. The quality of the model predicted output is quantified using the normalized mean-square error (NMSE), given as

$$\text{NMSE} = \sqrt{\frac{\sum(\hat{y}(k) - y(k))^2}{\sum(y(k) - \bar{y}(k))^2}} \quad (11)$$

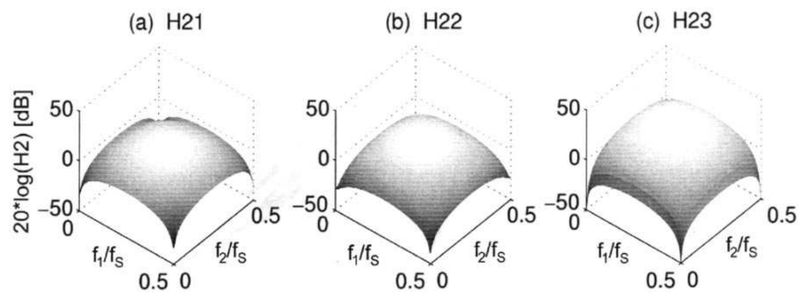

Fig. 6. GFRF $H_2(j\omega_1, j\omega_2)$ for (a) u_1; (b) u_2; (c) u_3 in (10).

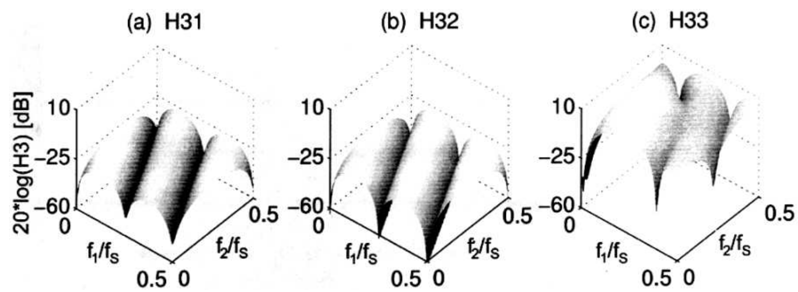

Fig. 7. GFRF $H_3(j\omega_1, j\omega_2, j\omega_1)$ for (a) u_1; (b) u_2; (c) u_3 in (10).

where $\hat{y}(k)$ is the model predicted output, $y(k)$ is the measured value and $\bar{y}(k)$ is the mean value of the measured output. For the example analyzed, the NMSE value was 0.3%.

It is important to emphasise that one single Volterra model cannot represent this system and any attempt to find such a model results in very poor model predictions. But by using the response spectrum map to determine an appropriate input and then by estimating in this case three SISO models and combining these gives the final MISO Volterra representation. The result is that now the MISO model should be an excellent representation of the system with the advantage that the properties, analysis and interpretation of this model can now be studied using all the methods developed for Volterra systems. But now these can be applied to severely nonlinear systems and to study subharmonic phenomena.

The Volterra kernels of the MISO model (7)–(9) can now be analyzed in the frequency domain. There are no cross-product terms between individual input components, and the model (10) can be considered to be composed of three independent submodels, one for each input component. By applying the probing method to the submodels (7)–(9), following the methodology given in Peyton Jones and Billings [13] the GFRFs are derived next, one for each submodel. There will be three different linear functions $H_1(j\omega)$, three different functions $H_2(j\omega_1, j\omega_2)$, etc. The linear functions $H_1(j\omega)$ are given in Fig. 5, where frequency of 0.5 is equal to the Nyguist frequency, which in this case is $1/(2T_s) = 9.54$ Hz.

For all input components, the functions $H_1(\omega)$ have the same parabolic shape for the magnitude, with different maximum values at the normalized frequency $f_1 = 0.25$. The functions $H_2(j\omega_1, j\omega_2)$ are given in Fig. 6. These also have a similar shape, with a maximum at $f_1 = f_2 = 0.25$. The functions $H_3(j\omega_1, j\omega_2, j\omega_3)$ are represented in Fig. 7, for the section $f_1 = f_3$. Again, the first two of these have similar features, with high magnitudes for $f_1 + f_2 + f_3 = 0.25$ and a minimum magnitude for $f_1 + f_2 + f_3 = 0$. Only for the third subsystem are the lines somewhat distorted, showing high magnitude for $f_1 + f_2 + f_3 = 0$ and a minimum magnitude on the frequency lines $f_1 + f_2 + f_3 = 0.25$, which is the direct opposite to the first two third-order frequency-response functions.

B. Example 2: Duffing–Holmes Equation

In this section, the Duffing equation is considered in the form also known as the Duffing–Holmes model

$$\ddot{y} + 1.5\dot{y} - y + y^3 = A\cos(t). \tag{12}$$

This equation was simulated using a fourth-order Runge-Kutta algorithm with an integration interval of $\pi/15$, for an amplitude A varying in the range $1 \leq A \leq 1.6$. The bifurcation diagram and the response spectrum map given in Fig. 8 shows cascades of period doubling, for different amplitudes of the input signal varying in the range $1 \leq A \leq 1.6$. In this example, the subharmonic of order $1/n = 1/2$ at 0.089 Hz obtained for amplitude $A = 1.2$ in the model (12) will be considered.

As in the previous example, a modified input is produced first. The modified input is generated from the original input signal, knowing the order of the subharmonic n and the time period T. By examining the response spectrum map given in Fig. 8, the parameters n and T can be obtained. For the amplitude value $A = 1.2$, the order is $n = 2$ and the time period is $T = 2\pi = 6.28$s. The original and the modified two-dimensional input signals are given in Fig. 9. For a system with the input $[u_1; u_2]$ represented in Fig. 9 a discrete-time MISO Volterra model was identified, using the MIMO OLS method

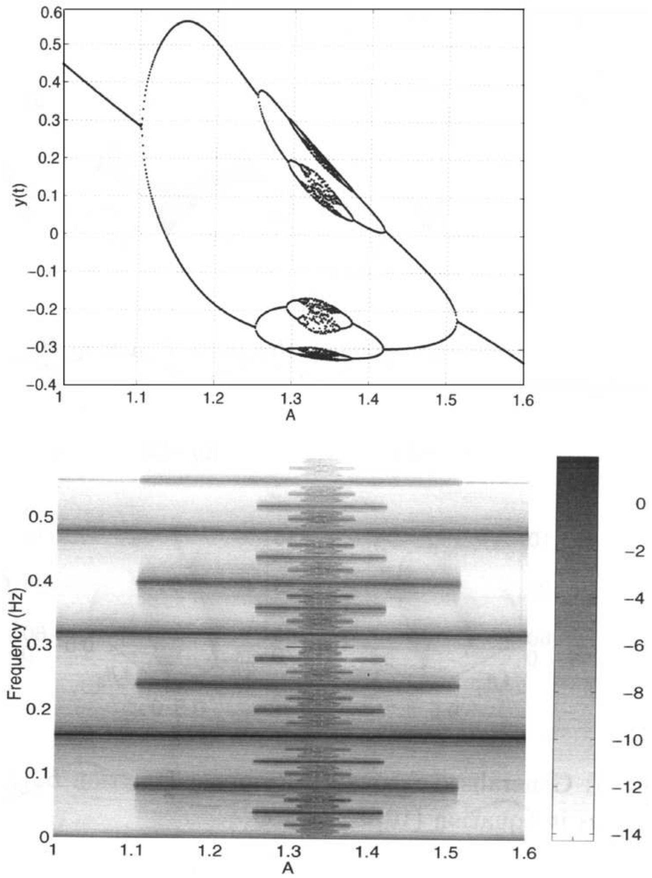

Fig. 8. Bifurcation diagram and response spectrum map (plan view) for the Duffing–Holmes (12).

[2]. The Volterra model selected had a third order of nonlinearity and no cross-product input terms (no terms of the type $u_1 u_2$)

$$\begin{aligned} y_1(k) = &\, 5.6235u_1(k-3) - 0.0859u_1^3(k-3) \\ &+ 2.9122u_1(k-1) - 0.0833u_1^3(k-1) \\ &+ 5.7643u_1(k-2)u_1(k-3) \\ &- 12.0268u_1(k-1)u_1(k-2) \\ &- 7.9389u_1(k-2) + 5.7980u_1^2(k-1) \\ &- 3.0893u_1^2(k-3) + 3.6287u_1^2(k-2) \end{aligned} \tag{13}$$

$$\begin{aligned} y_2(k) = &\, 14.6176u_2(k-1)u_2(k-2) + 6.6054u_2^2(k-3) \\ &+ 6.0183u_2(k-3) - 10.1978u_2(k-2) \\ &+ 0.4071u_2(k-2)u_2^2(k-1) - 7.8590u_2^2(k-1) \\ &+ 0.4472 - 13.5093u_2(k-2)u_2(k-3) \\ &- 0.3316u_2^3(k-1) + 4.0732u_2(k-1) \end{aligned} \tag{14}$$

where

$$y(k) = y_1(k) + y_2(k). \tag{15}$$

As in the preceding example, the model predicted output was estimated and used for model validation. Fig. 10 shows a good agreement between the original and the estimated output, for an NMSE value of 0.02%. In Fig. 10, the original input signal is also shown, with a period 2 times smaller than the resulting subharmonic. The Volterra model (15) has no cross-product terms between individual input components, therefore, the Volterra

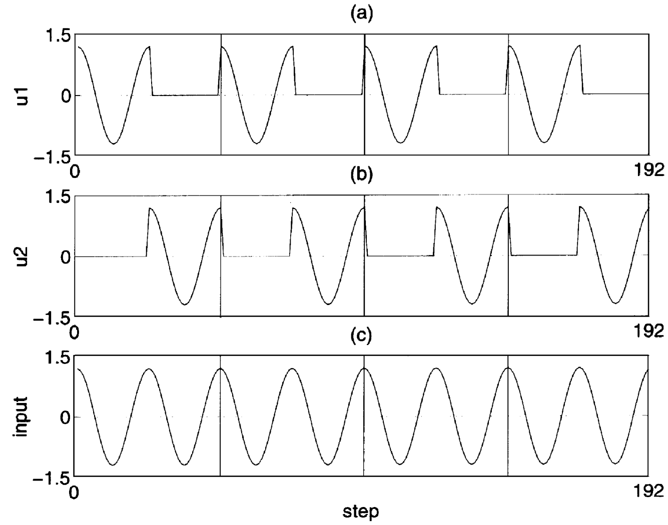

Fig. 9. Modified input signal $[u_1; u_2]$ with the components: (a) u_1; (b) u_2; (c) original input.

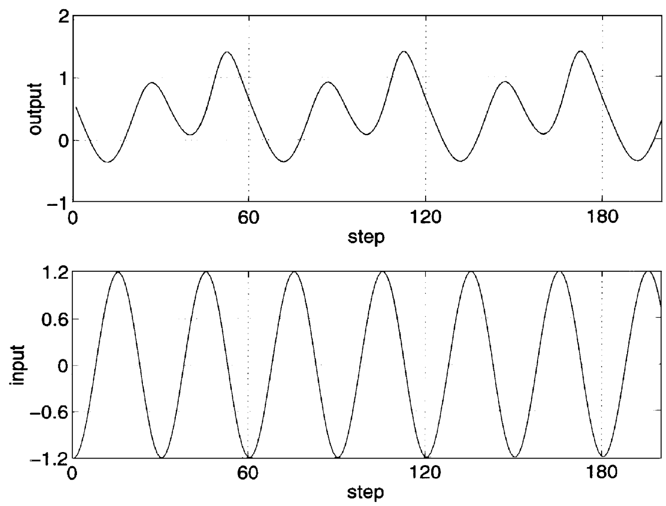

Fig. 10. Model (15) predicted output (dashed line), original output (solid line), and input signal.

kernels can be further analyzed in the frequency domain. By applying the probing method to the submodels (13)–(14), following the methodology given in Peyton, Jones, and Billings [13], the GFRFs are derived next, one for each submodel. The first-order GFRFs are given in Fig. 11, where the frequency of 0.5 is equal to the Nyguist frequency, which in this case is $1/(2T_s) = 2.38$Hz.

The functions $H_1(j\omega)$ have the same parabolic shape for both input components, with different maximum values, of 24 and 26 dB, respectively, at the normalized frequency $f_1 = 0.5$. They are also similar to the left hand side half of the functions $H_1(j\omega)$ derived in the previous example, given in Fig. 5. The functions $H_2(j\omega_1, j\omega_2)$ are given in Fig. 12. The shape of the functions $H_2(j\omega_1, j\omega_2)$ are again very similar. Both functions $H_2(j\omega_1, j\omega_2)$ have a maximum amplitude near $f_1 = f_2 = 0.5$ of 27 and 31 dB, respectively, and a minimum near the origin of the input frequencies.

The functions $H_3(j\omega_1, j\omega_2, j\omega_3)$ are represented in Fig. 13, for the section $f_1 = f_3$. For the first model, the function

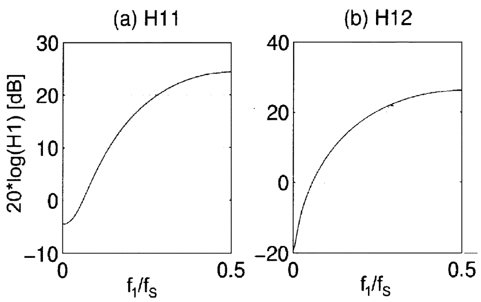

Fig. 11. GFRFs $H_1(j\omega)$ for (a) u_1 (b) u_2 in (15).

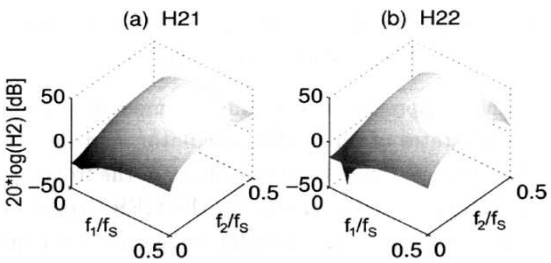

Fig. 12. GFRFs $H_2(j\omega_1, j\omega_2)$ for input (a) u_1, (b) u_2 in (15).

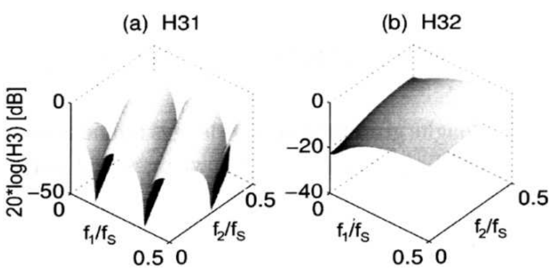

Fig. 13. GFRFs $H_3(j\omega_1, j\omega_2, j\omega_1)$ for input (a) u_1, (b) u_2 in (15).

$H_3(j\omega_1, j\omega_2, j\omega_1)$ shows high magnitude for $f_1+f_2+f_3 = 0.5$ normalized frequency, with a maximum value of -15dB, and a minimum magnitude is produced when $f_1 + f_2 + f_3 = 0.25$. For the second model, the function $H_3(j\omega_1, j\omega_1)$ shows a maximum magnitude of -2dB for $f_1 = f_2 = f_3 = 0.5$ normalized frequency and a minimum magnitude is produced when $f_1 = f_2 = f_3 = 0$. By comparing the maximum values of the GFRFs it is apparent that the significance of the nonlinearities in the model decreases with the order.

The frequency-response functions obtained in both examples have graphical representations with similar features. This may suggest that the H's previously derived correspond not only to the local Volterra kernels, but they can also be related to the original underlying system, which is the Duffing equation, and are therefore a global feature. This idea can be the starting point for further investigations into subharmonic analysis.

V. Conclusions

Mildly nonlinear systems can be studied by analysing just the first few terms in the Volterra series. In these cases inspection of the kernel plots or the equivalent GFRFs provides a complete characterization of the system properties. However, the Volterra series has limitations and it can only be used to model severely nonlinear systems around the equilibrium points within a relatively small area of convergence. Outside the Volterra convergence area, the nonlinear system dynamics can be much more complex. Phenomena associated with strong nonlinearities are generated including limit cycles, subharmonics and chaos.

The objective of this paper was to investigate the modeling, analysis and interpretation of nonlinear systems with subharmonics. A new modeling approach was introduced based on a MISO Volterra series model representation. The advantage of this approach is that it is relatively simple to apply and once the model has been obtained all the well known methods of analysis for Volterra series, which have until now been restricted to mildly nonlinear systems only, can now be applied to nonlinear systems which exhibit subharmonics.

The new approach was applied to modeling subharmonics associated with various steady states of the Duffing oscillator, and the GFRFs of the MISO models were used to analyze the system properties in the frequency domain. It was interesting to find common characteristics in the GFRF representations for different local subharmonics of the Duffing oscillator, suggesting that the GFRFs derived describe some invariant features of the system and not just the local behavior. This idea can form the starting point for further investigations into the analysis of systems with subharmonics.

References

[1] S. A. Billings and O. M. Boaghe, "The response spectrum map, a frequency domain equivalent to the bifurcation diagram," *Int. J. Bifurcation Chaos*, vol. 11, no. 7, pp. 1961–1975, 2001.

[2] S. A. Billings, S. Chen, and M. J. Korenberg, "Identification of MIMO nonlinear systems using a forward regressor orthogonal estimator," *Int. J. Contr.*, vol. 49, no. 6, pp. 2157–2189, 1989.

[3] S. Boyd, L. O. Chua, and C. A. Desoer, "Analytical foundations of Volterra series," *IMA J. Math. Contr. Inform.*, vol. 1, pp. 243–282, 1984.

[4] S. Boyd and L. O. Chua, "Fading memory and the problem of approximating nonlinear operators with Volterra series," *IEEE Trans. Circuits Syst.*, vol. CAS-32, pp. 1150–1161, Nov. 1985.

[5] L. O. Chua and C. Y. Ng, "Frequency domain analysis of nonlinear systems: formulation of transfer functions," *Electron. Circuits Syst.*, vol. 3, no. 6, pp. 257–269, 1979.

[6] M. J. Feigenbaum, "Universal behavior in nonlinear systems," *Los Alamos Science*, vol. 1, pp. 4–27, 1980.

[7] D. A. George, "Continuous Nonlinear Systems," MIT Research Lab. of Electronics, Cambridge, MA, Tech. Rep. 355, 1959.

[8] J. Guckenheimer and P. Holmes, *Nonlinear Oscillations, Dynamical Systems and Bifurcation of Vector Fields*. New-York: Springer-Verlag, 1983.

[9] Y. Ishida, T. Yamamoto, and S. Murakami, "Nonstationary vibration of a rotating shaft with nonlinear spring characteristic during acceleration through a critical speed—(a critical speed of a 1/3-order subharmonic oscillation)," *JSME Int. J. Ser. III*, vol. 35, no. 3, pp. 360–368, 1992.

[10] Y. Ishida, "Nonlinear vibrations and chaos in rotordynamics," *JSME Int. J. Ser. C*, vol. 37, no. 2, pp. 237–245, 1994.

[11] S. Lefschetz, "Linear and nonlinear oscillations," in *Modern Mathematics for the Engineer*. New York: McGraw-Hill, 1956, pp. 7–30.

[12] A. H. Nayfeh and D. T. Mook, *Nonlinear Oscillations*. New York: Wiley, 1979.

[13] J. C. Peyton-Jones and S. A. Billings, "Recursive algorithm for computing the frequency response of a class of nonlinear difference equation models," *Int. J. Contr.*, vol. 50, no. 5, 1989.

[14] S. S. Rao, *Mechanical Vibrations*. New York: Addison-Wesley, 1995.

[15] I. W. Sandberg, "Nonlinear input-output maps and approximate representations," *AT&T Tech. J.*, vol. 64, no. 8, pp. 1967–1983, 1985.

[16] J. M. T. Thompson and H. B. Stewart, *Nonlinear Dynamics and Chaos*. New York: Wiley, 1991.

[17] N. Wiener, *Nonlinear Problems in Random Theory*. New York: Wiley, 1958.

[18] M. J. Feigenbaum, "Universal behavior in nonlinear systems," in *Universality in Chaos*, P.Predrag Cvitanovic, Ed. Bristol, U.K.: Adam Hilger , 1989, pp. 49–84.

Otilia M. Boaghe received the engineering diploma in electronic and computer engineering from the Transilvania University, Brasov, Romania, in 1995, and the M.Sc. (with distinction), and the Ph.D. degrees, from the University of Sheffield, Sheffield, U.K., in 1996, and 2000, respectively.

She is currently employed as an IC Development Engineer at Philips Semiconductors, Zurich, Switzerland. Her research interests in the field of systems engineering include nonlinear system analysis, Volterra series, system identification, spectral analysis, neural networks, wavelets, subharmonics, wave-force dynamics, and geomagnetic activity.

Stephen A. Billings received the B.Eng. degree in electrical engineering (with first class honors) from the University of Liverpool, Liverpool, U.K., in 1972, the Ph.D. degree in control systems engineering from the University of Sheffield, Sheffield, U.K., in 1976, and the D.Eng. degree from the University of Liverpool, Liverpool, U.K., in 1990.

In 1990, he was appointed as a Professor in the Department of Automatic Control and Systems Engineering, University of Sheffield, and leads the Signal Processing and Complex Systems Research Group. His research interests include system identification and information processing for nonlinear systems, narmax methods, model validation, prediction, spectral analysis, adaptive systems, nonlinear systems analysis and design, neural networks, wavelets, fractals, machine vision, cellular automata, spatio-temporal systems, fMRI, and optical imagery of the brain.

Dr. Billing is a Chartered Engineer [CEng], Chartered Mathematician [CMath], Fellow of the Institution for Electrical Engineers, U.K, and Fellow of the Institute of Mathematics and its Applications.